
NIM BASED MUON TELESCOPE – AN EDUCATIONAL EXPERIMENT FOR POST GRADUATE STUDENTS

S.N.L Sirisha¹, Kajal Garg² and Sonali Bhatnagar³

^{1,2}Research Scholar
Dayalbagh Educational Institute
Agra282110, India.

³Department of Physics and Computer Science
Dayalbagh Educational Institute
Agra282110, India.

(Submitted: 04-12-2014)

Abstract

Cosmic rays offer an outstanding educational platform involving a free source of high energy subatomic particles. In continuation of the preliminary studies [1] presented at 31st National Conference of Indian Association for Radiation Protection at BARC, the paper demonstrates the fundamental properties of cosmic rays and also exposes the post graduate (PG) students to particle detection techniques, advanced nuclear electronics and data analysis. A review on several possible studies using plastic scintillator such as time characteristics of PMT which includes rise time, fall time, amplitude dependence on high voltage, jitter and walk effects of PMT pulse, coincidence, horizontal and vertical separation between detectors, dependence of cosmic ray flux with respect to temperature, pressure, humidity will be discussed.

1. Introduction

In recent years, a numerous number of high schools and universities are forming collaborations (for e.g.: CROP (Cosmic Ray Observatory Project)[2], CHICOS (California High School Cosmic ray ObServatory)[3], SEASA (Stockholm Educational Air Shower Array)[4], ALTA (Alberta Large Area Time-Coincidence Array)[5]) for performing the cosmic ray studies all over the world. Many educational aspects tend to characterize the experiments using different detection techniques for study of fundamental properties of high energy particles. This has also

offered a possible usage of the advanced nuclear laboratory which involves construction of apparatus, use of different detectors, physical measurements, muon monitoring, data analysis and interpretation for students in field of high energy physics.

In the past few years there have been some impressive advances in our understanding of Ultra High Energy Cosmic Rays (UHECR's). The origin of UHECR's is a challenge for observational/experimental studies of particle acceleration and its propagation which provides

information on the spectrum, chemical composition and anisotropy.

Cosmic rays (CRs) are particles originating from space which bombard the Earth's atmosphere. The spectrum of relativistic particles has been observed ranging from 10^6 eV to 10^{19} eV [6]. It is described by a power law which slightly steepens at 3×10^{15} eV which is termed as 'knee' and the spectrum flattens down at the ankle near 3×10^{18} eV. The knee may be the result of limitations on particle acceleration at typical supernovae, whereas the ankle may indicate a transition to particles of extragalactic origin. HiRes (High Resolution Fly Eye's) [7] and Telescope Array [8] claim the detection of the GZK feature and is consistent with the value of $E_{1/2}$, i.e. the energy at which the modification factor in the flux of UHECRs is reduced to $\frac{1}{2}$ of the value inferred from the lower energy extrapolation, can be used as a powerful indicator of the presence of GZK feature and its association to photo-pion production. It measured the quantity and found its value to be $10^{19.73 \pm 0.07}$ eV. The chemical composition measured by HiRes by using elongation rate is consistent with a proton dominated composition at energies above 10^{18} eV. Pierre Auger Observatory [10] measured and observed a gradual change in composition at higher energies which is dominated by iron at 50 EeV. It also found the correlation of the arrival direction of UHECRs above 57 EeV. But it is difficult to infer the flux reduction at 10^{19} eV. Overview of the cosmic ray spectrum obtained from various observatories such as LEAP [11], AKENO [12], AUGER [13], KASCADE [14], AGASA [15], HiRes and Proton is shown in Figure 1.

The quest of UHECRs is related to the issue of transition from Galactic cosmic rays to CRs generated in extragalactic sources. It has been considered that the ankle in the CR spectrum, at $\sim 10^{19}$ eV, is the spectral signature of the transition from a steep Galactic spectrum to a flatter extragalactic spectrum. The nature of the ankle is the consequence of three models developed. The *dip model* [16] explains the spectrum of cosmic

rays propagating on cosmological scales due to Bethe-Heitler pair production. The *mixed composition model* [17] describes that larger abundances of nuclei is heavier than hydrogen. The maximum energy of protons is relatively low at $\sim 4 \times 10^{18}$ eV and for iron it extends to 10^{20} eV. This is considered as disappointing fit due to flux suppression at 10^{20} eV with intrinsic cutoff at source spectrum and no correlation due to heavy composition at highest energy. Both these models i.e. *dip and mixed composition* lead us to expect that galactic cosmic ray ends in EeV region rather than ankle. This is even supported from the cosmic anisotropy studies. This is due to the supernovae remnant (SNR) [18] paradigm which is based on non-linear theory of particle acceleration at supernova shocks where cosmic ray acceleration in SNRs may reach a maximum rigidity $\sim 10^{16}$ GeV. The main discrimination among these models is based on the measurement of chemical composition especially in transition region.

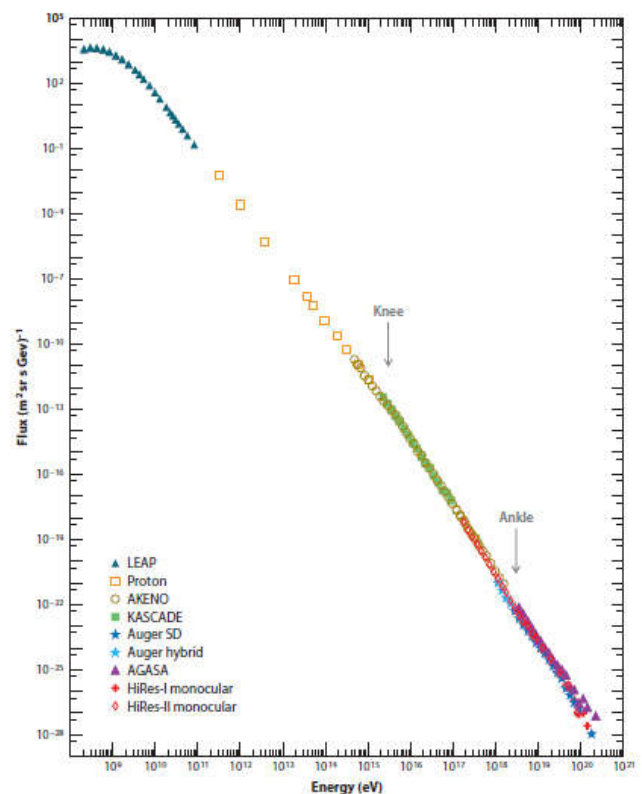
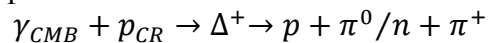


Figure 1: Cosmic Ray Spectrum [18]

The study of arrival distribution of the high energy cosmic rays is the most useful method for identifying the sources. This forms different categories: a) search for source of galactic central region, b) significant correlation of cosmic ray arrival direction with astrophysical objects, c) Cosmic ray arrival direction distribution for its anisotropy search.

At energies below 10^{14} eV, the spectrum can be measured directly by balloon and satellite-borne experiments. These experiments generally have an area of less than 1 m^2 . Above this energy, the flux is generally too small to make direct measurements. Ground-based experiments are used, where the energy of the primary cosmic ray must be inferred from its secondary's which are produced after the interaction of primary source with the Earth's atmosphere. The high energy primary cosmic rays are protons. These protons interact through the cosmic microwave background (CMB) [19] photons on their way to the earth. Above threshold energy, the following photo-production interaction is allowed:



where the number of protons should significantly decrease. This energy is referred to as the Greisen-Zapsepin-Kuzmin (GZK) cut-off and corresponds to proton energy of $\sim 4 \times 10^{19}$ eV. Protons above this range will interact with the CMB photons and have their energy degraded while producing an air shower cascade which is mostly of charged and neutral pions. These particles will subsequently decay or interact with other nuclei. The air shower has three components: electromagnetic (80%), muonic (1.7%) and hadronic (0.3%) [20]. Neutrinos are not counted, although they are abundantly produced in weak decays. Relativistic charged particles will produce Cerenkov light as they propagate through the atmosphere. Finally, excitations of nitrogen molecules in the atmosphere will generate fluorescence light.

Measurements of multiparticle production in fixed target experiments at low energy and in collider experiments at high energy are suitable to verify model assumptions and to limit their extrapolations

to cosmic ray energies. The data which reaches upto 10^{17} eV [21] equivalent energy of cosmic ray protons obtained from LHC is of more important. The high energy secondary particles are more relevant to interpretation of cosmic ray data. Muon detection is an essential part in the Large Hadron Collider (LHC) experiments. It helps in understanding the background of the underground detectors and to simulate the atmospheric showers induced by muons. At super high energies, these are also considered for exploration of primary cosmic rays, neutrino studies in different arrays like Super-Kamiokande [22], GRAPES-3 (Gamma Ray Astronomy at PeV Energies) [23] and for numerous environmental experiments like the solar activity characterization or climate change observations [24]. Also, it has successfully been used as muon tomography technique in the search for hidden rooms in pyramids or in volcanology [25]. There are other possible applications to increase the safety procedures in mining excavations, oil industry as an easy way to search for oil bags or at the customs checkpoints, to scan the passing vehicles [26]. In many applications such as industry and academia, an accurate determination of the direction from where gamma rays are emitted is either needed or desirable. Radiation therapy treatments, the search for unknown sources, and homeland security applications are few of the fields that can benefit from directional sensitivity to gamma-radiation [27].

This paper is extension of the previous work done on "Preliminary Studies of Muon Telescope" [1]. We discussed till now the fundamental properties of cosmic ray spectrum, its chemical composition and anisotropy. In section II, we present a brief description of on-going experiments in our laboratory where the PG students get an exposure to advanced nuclear electronics. The feedback of the students who did the lab course work is discussed in section III. An overview of various methods that can be implemented for study of time characteristics of photomultiplier tube, obtain the efficiency of detector system through coincidence techniques, calibrate the TDC and obtain the

energy deposited from CAMAC modules (ADC, TDC), angular dependence of cosmic ray flux and finally ends with atmospheric parameters such as temperature, pressure, solar activity and their effect on cosmic ray flux are presented in Section IV. The future aspects of our laboratory are given in Section V.

2. Experiments conducted with Post Graduate Students:

In the preceding work, we performed basic pre-preliminary studies of our telescope. It includes light leakage testing from detectors and optimized the discriminator threshold voltage. Counting statistics was applied to determine the error flexibility within the data range. The experimental studies conducted with the students for understanding the concept of scintillation, signal transmission, electronics used to suppress the noise, logical conversion of pulse to acquire data in optimizing PMT operating voltage and the correlation between count rate and accidentals will be discussed in this section. Two polystyrene (PS) based scintillators i.e. Double Fiber Detector (DFD) and Single Fiber Detector (SFD) with dimension $24 \times 23.5 \times 2 \text{ cm}^3$ are presently in use in the laboratory. These were assembled at Cosmic Ray laboratory, Ooty; a field station of T.I.F.R, Mumbai. Polystyrene (PS) with a photon emission at 300 nm is doped with a two stage phosphor wavelength shifter composed of 0.5% p-terphenyl (absorbs photon at 300 nm and emits at 350 nm) and 0.02% POPOP (absorbs photon at 350 nm and emits at 410 nm). The response peak of the organic scintillator is shown in figure 2.

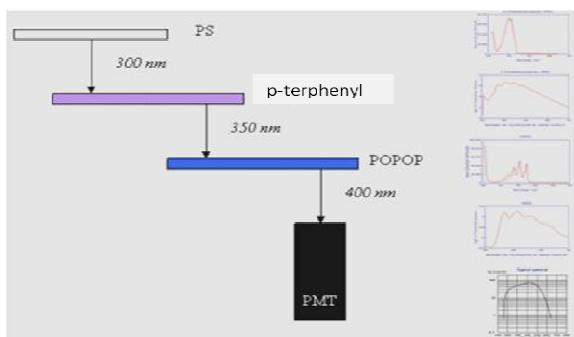


Figure 2: Organic Scintillator Mechanism [8].

During the process of polymerization the temperature should be controlled at 70°C for at least 60-72 hours. Polymerization is a highly exothermic process (165 cal/gm) and the temperature control is mandatory when dealing with large volumes. Rising polymerization temperature may produce bubbles and cracks. The fabricated scintillator is shown in figure 3 (a).



Figure 3(a): Plastic Scintillator used in Experiment.

After cleaning the scintillator with isopropanol liquid and polish on both extremes with sandpaper, the scintillator is grooved all over. Wave length shifting (WLS) fiber of Kuraray Y-11 manufacture (refractive index, $n=1.59$, inner clad, $n=1.42$, outer clad, $n=1.49$) with double-clad of 1.2 mm diameter is inserted into the groove. This absorbs the primary scintillation light ($\sim 410 \text{ nm}$) and reradiates the energy at a longer wavelength ($\sim 550 \text{ nm}$) [4]. It helps to match the emission spectrum of scintillator with the response peak of a photomultiplier tube. They also increase the decay time, improve the resolution and decreases the self-absorption of the detector. The scintillation detectors embedded with wavelength shifting fibers are optically coupled to photomultiplier tube (ET Enterprises, Type 9807B), a regular 12-stage linear focused dynode structure and highly efficient at 550 nm. An aluminum box with volume 55 cm^3 (length) \times 25 cm (width) \times 10 cm (height) and 1.2 mm in thickness is designed to place the entire setup i.e. scintillator coupled to a photomultiplier tube using a cookie (figure 3(b)). The whole setup of detector is shown in figure 3(c).

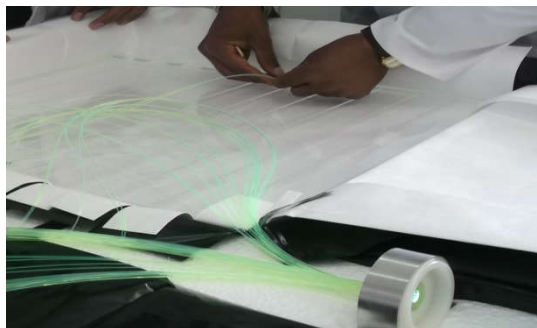


Figure 3(b): Optical coupling of scintillator to PMT with a cookie.



Figure 3(c): Detector Setup

The information provided by the detectors from the emitted radiations is in the form of electrical signals. This is processed by a signal processing electronics using Nuclear Instrumentation Module (NIM) which can sort out various unwanted signals from detectors to extract energy information and determine the relative timing between the two signals. It generates a fast negative logic with a rise time of the order ~ 1 ns. The corresponding voltage levels are thus 0V and -0.8V for logic 0 or 1 respectively. These fast NIM signals can be transmitted through coaxial cables. Students have studied the characteristics of pulse, coaxial cables, impedance matching, inhibiting discriminator pulse from veto functioning, versatile functions of logic unit such as AND, OR and anti-coincidence. Correlation between detector count rate and its accidental rate is also observed. These are briefly described along with the results in the following exercises given below:

Exercise 1: Study the pulse characteristics

In any pulse processing system, it is important to distinguish between two types of signal pulses i.e. linear and logic. A linear pulse carries information through its amplitude or shape. A sequence of these pulses differs widely by its size and shape characteristics. Logic pulse has a standard size and shape that carries information only by its presence or absence or by precise time of its appearance. Initially all radiation detector signal starts out with linear pulses and at some point, a conversion is made to logic pulses based on some pre-determined criteria.

A fast linear pulse collects the output current of radiation detector using a collection circuit whose time constant is small. The signal-to-noise ratio properties of fast linear pulses are always much less than a corresponding tail pulse which is derived by integrating the charge output of the detector across a large time constant [28]. The rapid rise and fall time overcome this outcome when timing information and high counting rates are more important than amplitude resolution. Its polarity depends on the bias voltage applied to the detector. The basic pulse characteristics associated with its polarity, amplitude, shape and its occurrence in relative time are explained here for a linear and NIM logic pulse to study its voltage/current as function of time. Figures 4(a) and 4(b) demonstrate these parameters obtained for double and single fiber detector configurations.



Figure 4(a): Linear pulse characteristics obtained for double fiber detector.



Figure 4(b): Linear pulse characteristics obtained for single fiber detector

Both the configurations are compared in order to understand the amplitude difference where a 350 mV amplitude pulse generated for double fiber, 200 mV in case of single fiber detector. This depends on the number of photoelectrons that reach the anode of the PMT where these fiber configurations may give a possible impact.

Exercise 2:(a) Check the reflections in a cable by using a 50Ω impedance terminator.

Signal transmission is transfer of a signal from point A to B and also to preserve the information in the signal. These cables should be capable of transmitting an infinite frequency range over a certain distance in uniform and coherent manner. But stray capacitances, inductance or resistance will invariably results in distortion of the pulse at receiving end. When a fast pulse signal is transmitted through simple wire connections, it attenuates and dies down after few cm. It is necessary to transmit infinite range of frequencies in laboratory. A basic concept in processing of pulses from radiation detectors is the impedance of the devices that comprise the signal processing chain. High input impedance usually has a less load [29]. For example, the input impedance of an oscilloscope is always high to avoid excessive loading.

The device impedance also should be in match with the cable impedance to avoid signal distortion from reflection. When a fast signal is viewed on an oscilloscope, it undergoes an

impedance mismatch due to high impedance of oscilloscope. In such cases, the cable can be terminated with an appropriate value so as to adjust the total load impedance seen by cable. This is done by placing a resistance of 50Ω in parallel with device. The signal seen by the oscilloscope for DFD and SFD are shown in figure 5. The signal is reflection free on terminating with 50Ω load impedance.

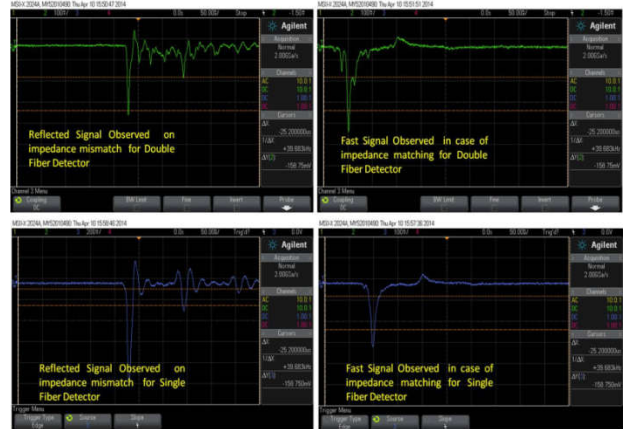


Figure 5: Analog Signal Transmission Observed using with and without 50 Ω terminating.

We can observe from figure 5, that the signal distortion from reflection can be avoided by matching device impedance with cable impedance. Direct transmit of fast NIM signal will result in impedance mismatch and fast signal reading. But slow signal can be transmitted and also compatible as cables are not too long. So cable should be terminated for fast NIM pulse.

(b) To compute the characteristic impedance, velocity propagation, time delay and reflection coefficient of coaxial cables RG 59/U, 5D2V.

Coaxial cables are used for standard transmission of signals. It consists of two concentric cylindrical conductors separated by a dielectric material. The outer conductor serves as a ground and also shields the central wire from stray electromagnetic fields. Frequencies ≤ 100 kHz are efficiently attenuated in most standard cables [28]. The line constituents of coaxial cables generally contain a self-capacitance and inductance. Using EM theory

for two concentric cylinders, they can be represented as:

$$L = \frac{\mu \ln\left(\frac{b}{a}\right)}{2\pi} (H/m) = 0.2k_m \ln\left(\frac{b}{a}\right) \mu H/m$$

$$C = \frac{2\pi\epsilon}{\ln\left(\frac{b}{a}\right)} F/m = \frac{55.6k_e}{\ln\left(\frac{b}{a}\right)} pF/m$$

Where a,b are radii of inner and outer cylinders; μ , ϵ are permeability and permittivity of insulating dielectric; $k_e = \epsilon/\epsilon_0$, $k_m = \mu/\mu_0$ permeability and permeability relative to vacuum. For non-ferromagnetic materials, $k_m=1$. L and C are on the order of 100 pF/m and few tenth $\mu H/m$. Coaxial cables with air or other gas as a dielectric have a propagation velocity very close to the velocity of light in a vacuum (3.00×10^8 m/s).

General wave equation for a coaxial cable in terms of transmission line can be represented as

$$\frac{\partial^2 V}{\partial z^2} = LC \frac{\partial^2 V}{\partial t^2} + (LG + RC) \frac{\partial V}{\partial t} + RGV$$

Let us consider an ideal loss less cable where R and G are zero

$$\frac{\partial^2 V}{\partial z^2} = LC \frac{\partial^2 V}{\partial t^2}$$

For a sinusoidal voltage in time

$$V = V(z) \exp(i\omega t)$$

$$\frac{\partial^2 V}{\partial z^2} = -\omega^2 LC V = -k^2 V$$

$$k^2 = \omega^2 LC$$

The space solutions to represent the two waves which are travelling in +z and opposite -z direction are

$$V(z, t) = V_1 \exp(i(\omega t - kz)) + V_2 \exp(i(\omega t + kz))$$

Here second wave corresponds to a reflection and its presence or absence depends on the boundary

for the cable. From the above equation, k is considered as wave number and velocity of propagation is

$$v = \frac{\omega}{k} = \frac{1}{\sqrt{LC}}$$

As long as the cable is constant in cross-section, the product LC is independent of length and $LC = \mu\epsilon$, where ϵ permittivity is and μ is permeability of dielectric. Thus for a cable with free space as dielectric velocity of propagation = $\frac{1}{\mu_0\epsilon_0} = c$ = speed of light in vacuum. Speed of signal propagation is also reciprocal of time of propagation per unit length which is also known as $T = v^{-1} = \sqrt{LC}$. Here is T is time delay of the cable per unit length of the order 5 ns for 50 Ω cable.

All signal cables generally utilize polyethylene for dielectric in which the velocity of propagation is about 66% of that of light in vacuum. In some delay cables it is reduced by a factor of 100 [29]. Pulse transmission through coaxial cable is in two extremes i.e. low frequency and slow pulses, high frequency and fast pulses. The application of fast and slow pulses depends on the comparison of fastest pulse component (rise time) with the transit time of the pulse. For dielectric material such as polyethylene, the transit time is about 5.1 ns/m [29]. Similarly a pulse through 15 m of RG 59/U coaxial cable has a transit time of 76.5 ns/15m. Pulsethrough high rise time compared with the transit time is considered as slow pulse. In this case, cable acts much like simple conductor. The resistance of central conductor is very small for cables less than 100 m length. When a 20 m RG-59/U cable have 0.5 μs rise time, the resultant pulse can be considered as a slow pulse. This is due to the transit time of the cable i.e. 102 ns/20m being less than the rise time. Thus, for a signal transmission of slow pulse through a cable does not any termination as the resistance of central conductor is very small which result in negligible signal loss. Characteristic Impedance is another important property of transmission cable which is ratio of the voltage to the current in the cable.

$$Z_o = \frac{V}{I} = \sqrt{\frac{L}{C}}$$

In fast nuclear electronics applications, cables have a standard characteristic impedance of 50 Ω and for slower spectroscopy pulse the characteristic impedance is 93Ω. These cables are limited to a range of 50-200 Ω of characteristic impedance. The ratio $\frac{b}{a}$ should be a factor of 3.6 to minimize losses. For all these cables, dielectric is Polyethylene whose relative permittivity is 2.29. The observations are given in the table 1 and

When reflections overlap with original signal, then interference or distortion will result. Reflections occur when a travelling wave encounters a new medium in which the speed of propagation is different. In transmission lines, these reflections occur when characteristic impedance of the line is suddenly changed. These reflections are calculated by considering boundary conditions at interface. Consider a cable of characteristic impedance Z terminated with an impedance R. As the signal travels, the ratio of voltage to current must be equal to Z. When the interface encounters reflections, it must be compatible with original characteristic impedance since they travel back in opposite direction. Thus

$$Z = \frac{V_o}{I_o}, R = \frac{V_o + V_r}{I_o + I_r} \Rightarrow Z = \frac{V_R}{-I_R}$$

V_o, I_o are voltage and current of original signal and V_R, I_R are voltage and current of reflected signal. From these equations, Reflection coefficient

$$\Gamma = \frac{V_R}{V_o} = \frac{-I_R}{I_o} = \frac{R + Z}{R - Z}$$

If $R > Z$, the reflection will be of same polarity, but with amplitude between 0 and original pulse height. For infinite load impedance, reflected amplitude is equal to incident amplitude. The reflection is in opposite polarity when $R < Z$. For zero load impedance, reflection is equal and opposite in polarity to incident amplitude. If $R = Z$, No reflection takes place where the load and cable impedance gets matched.

Exercise 3: Study the specifications of the Phillips 704 Discriminator: VETO, OUT.

Discriminator is a device that responds only to input signals with a pulse height greater than a certain threshold value. It gives a standard logic signal when the criterion gets satisfied. It blocks out low amplitude noise pulse from PMT and other detectors. Time arrival between input and output is constant where as an important aspect of

Table 1: Characteristic Impedance

Coaxial Cable	Outer diameter (mm)	Inner diameter (mm)	log (D/d)	ϵ_r	$Z_o(\Omega)$
Manufacturer Values RG59/U	4.95	0.8	0.79	2.29	75
RG 59/U	4.40	0.63	0.84	2.29	76.6 (2.3% error)
Manufacturer Values 5D2V	7.3	1.4	0.71	2.29	50
Coaxial Cables	5.01	0.79	0.75	2.29	50.1 (0.2% error)
Manufacturer RG 59/U		69	5.14		0.89
RG 59/U		73 (5% error)	5.18 (0.7% error)		0.92 (0.3% error)
Manufacturer 5D2V		65	5.06		0.78
5D2V		68 (4% error)	5.09 (0.5% error)		0.81 (0.3% error)

Signal in a coaxial cable is sum of original and reflected signal travelling in opposite direction. It is represented in arbitrary signal form as

$$V = f(x - vt) + g(x + vt)$$

discriminator is the method of triggering which is a leading edge triggering. It occurs the moment pulse crosses the threshold value. Double pulse resolution and continuous pulse train are two parameters of this module which measures the smallest time separation between two pulses and the highest frequency of equally spaced pulses [30]. A standardized NIM logic level (-800mV) pulse is delivered while suppressing the unwanted stray radiations arriving along with analog signal. Inhibiting the discriminator pulse can be accomplished by fast vetoing. This VETO function is shown in figure 6.



Figure 6: VETO Function in Model 704 Quad four channels Discriminator.

Although the main use of a discriminator is to turn a variable-height input pulse into a standard logic pulse, there are additional features of this unit that can be used. Each discriminator channel has a “complementary” output, noted as \overline{OUT} . This output is always opposite to the regular outputs as shown in Figure 7.

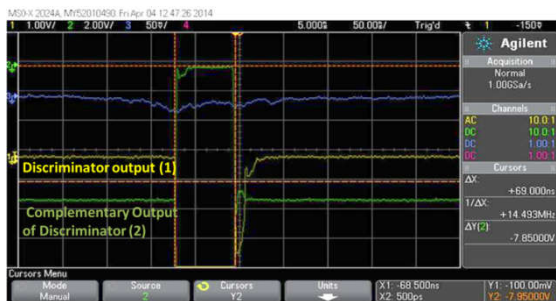


Figure 7: Discriminator Specification Study from Oscilloscope.

Exercise 4: Study the 2 input AND, OR logics using Phillips Quad Four fold logic unit.

The coincidence unit determines if two or more logic signals are coincident in time and generates a logic signal if **true (1)** and no signal if **false (0)**. Versatile functions of this module [31] with the selection of Logic AND, OR and Anti-coincidence are observed in figure 8(a), (b), (c).

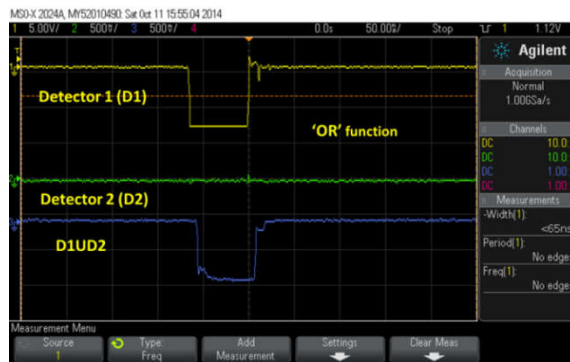


Figure 8(a): Logic OR function

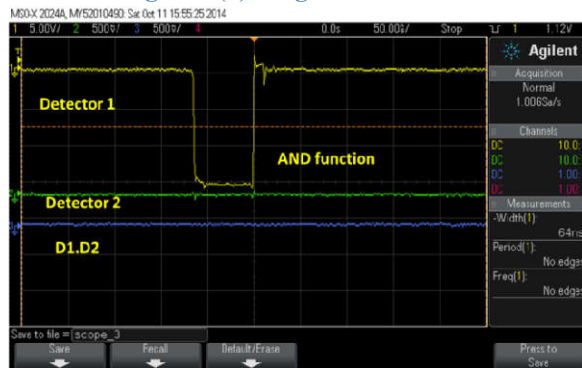


Figure 8(b): Logic AND function

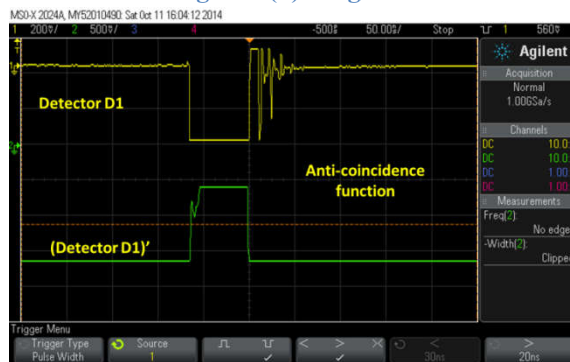


Figure 8(c): Anti-coincidence function

Figure 8(a) demonstrates the OR function where the status of detector D1 is 1 and D2 is 0 which results in an output as 1. This proves that the module performs OR logic. Similarly in figure

8(b), we can observe the AND logic i.e. when D1 is 1 and D2 is 0, the final output gives 0. Figure 8(c) shows the Anti-coincidence function when input (D1) is given.

Exercise 5: Determine the PMT (photo-multiplier tube) operating voltage and the count rate correlation with accidental counts in the detector.

To improve the acceptance value of plastic scintillator while suppressing the lower energy signals from PMT, the operating voltage for each detector i.e. (Double Fiber Detector, DFD and Single Fiber Detector, SFD) is determined. The experimental setup is shown in figure 9. Two plastic scintillation detectors are placed in coincidence. The threshold voltage of Quad 300 MHz discriminator (model number 708 [30]) was fixed at – 20 mV with a pulse width of 60 ns.

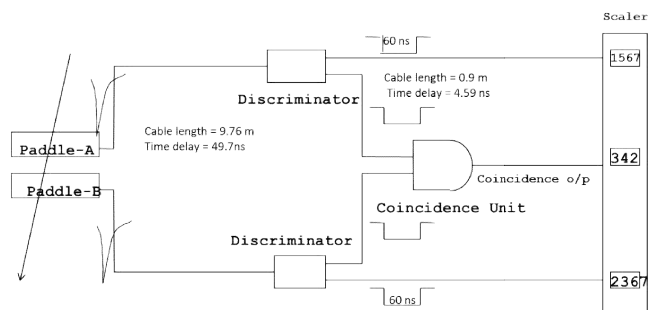


Figure 9: Experimental setup

The high voltage of one detector is fixed at 1700V whereas the high voltage of the other is varied from 1200 – 1800 V with 50V interval. To obtain a coincidence among the pulse the logic switch of Phillips Quad four fold logic unit (model number 756 [31]) is set at level 2. The counts were taken using the CAEN Quad Scaler and Preset Counter Timer (model number N1145 [32]). The coincidence rate/sec with respect to high voltage (H.V.) is observed for each PMT of the detector in order to determine its operating voltage.

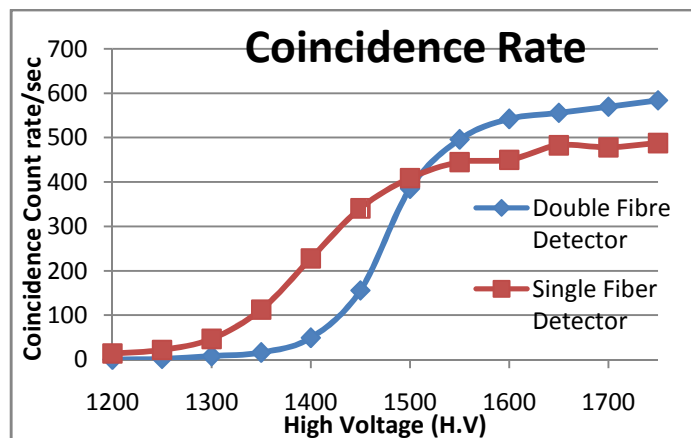


Figure 10: Operating voltage of PMT in DFD and SFD

From the plot (Figure 10), the operating voltage for each detector is observed at the point of inflexion for single fiber detector it is observed to be 1500V and for double fiber detector at 1550V. While making the coincidence measurement, we should consider the uncorrelated background events in the detector. They may arrive within the resolving time of the circuit or through random noise which triggers the discriminator. We can overcome this disadvantage by measuring the accidental coincidences that occur in circuit which must be kept to a minimum. The rate of accidentals can be estimated from the singles rate in each detector and the time resolution of the circuit. Consider n_1 and n_2 are the individual count rate for detector 1 and 2 respectively and τ is the resolution time which is set to trigger the circuit. Total number of accidentals per unit time,

$$A = 2\tau n_1 n_2,$$

Where τ is 60 ns. Correlation of detector count rate with accidental is shown in figures 11 (a), (b).

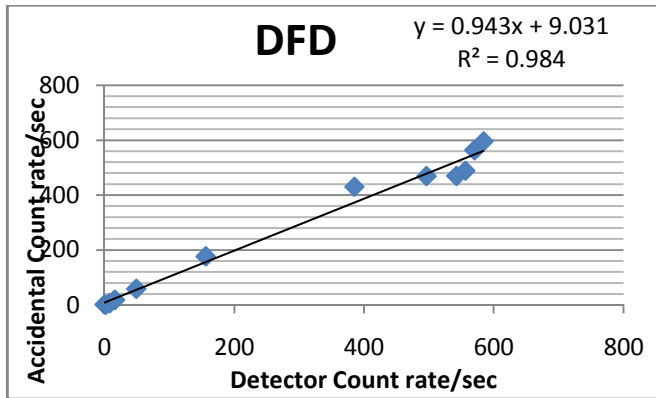
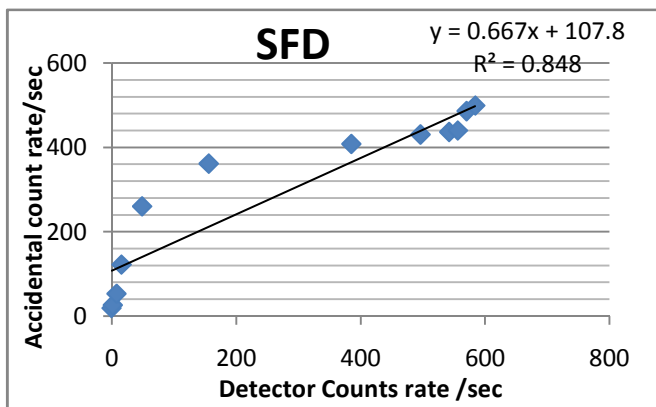


Figure 11(a): Correlation between detector count rate and accidentals in double fiber detector



11(b): Correlation between detector count and accidentals in fiber detector

Figure rate single

a	To a great extent
b.	Sufficient
c.	A bit
d.	Nothing

From figure 11 (a), (b); we can observe a linear relation with in the detector count rate and its accidentals. This is due to the noise which gradually increases with count rate on increasing the high voltage (H.V) of the PMT.

3. QUESTIONNAIRE FOR LABORATORY STUDENTS

After evaluation of the results we conducted an analysis through questionnaire regarding understanding capability of the students in

performing the experiment. The questionnaire helped us to understand the basic conceptual problems and evaluating the misunderstandings. At that point of view we prepared the following for students:

1. Did you understand the scintillation mechanism after doing the experiment?
2. Did you understand the main significance of PMT which is used in the experiment?
3. At PG level do you understand the working of this experiment?
4. Is the theoretical concept of coaxial cables clear which are used for transmission of fast pulse in the experiment?
5. Discriminator is used to suppress noise and give a standard logic signal. Do you think it acts as main source in experiment?
6. Did you understand why the signals are transmitted through Logic unit in experiment?
7. Interaction of radiation with matter. Is this concept which you studied in the graduation clear after performing the experiments in this laboratory?

The rating of the students opinion is taken through the following multiple choice options regarding their understanding capability in scintillation mechanism, PMT significance, coaxial cable transmission, discriminator, logic unit and experiment working with its concept clarity.

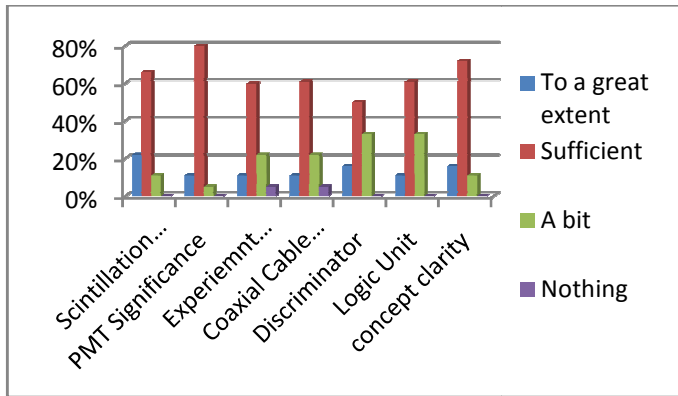


Figure 12: Students feedback in understanding the concepts of the experiemnt

Taking into account the students responses we concluded from graph (figure 12): 66% of students understood the scintillation mechanism, 83% got the significance of PMT, 61% understood the transmission concept in coaxial cables, 50% understood the working of discriminator where as 61% understood about logic gate usage in experiment and it is remarkable that 72% of the class got the clarity of working principle of experiment and its concept.

8. Among the experiments which is more user friendly

- a. GM counter
- b. NaI - Gamma ray spectroscopy
- c. NaI - Multichannel analyzer
- d. Plastic scintillator – Nuclear Instrumentation Module

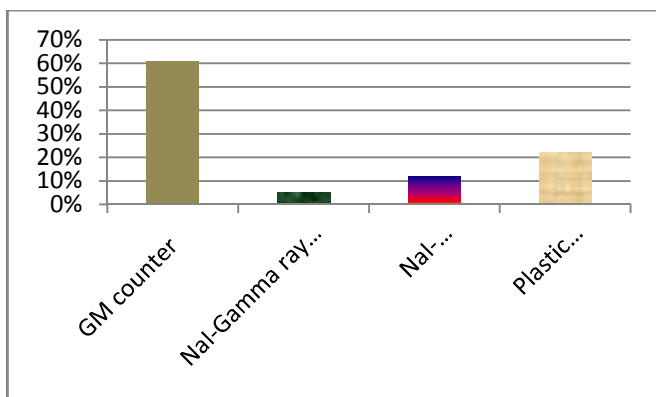


Figure 13: Students feedback after performing the experiments in the laboratory

Among the experiments which are performed by students in the laboratory, as shown in graph (figure 13), 61% of the students felt GM counter is more userfriendly where as it is remarkable that 22% of the class are comfort with the usage of NIM based plastic scintillator experiment which is presently studied in this paper.

9. Which one do you think is more preferable for study of cosmic rays?

- a. NaI
- b. Plastic Scintillator

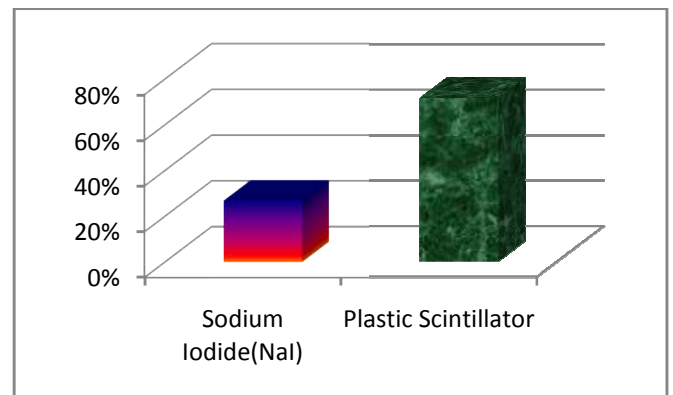


Figure 14: The feedback of students in using the plastic scintillator and Sodium Iodide (NaI) for study of cosmic rays

While comparing the organic and inorganic detectors (as shown in graph (figure 14)) which are present in laboratory for study of cosmic rays, 72% of the students opted for plastic scintillator which is suitable got cosmic ray study.

10. Among the techniques used, which is preferable for studying the efficiency of detectors

- a. Pulse Height Discrimination
- b. Coincidence Technique

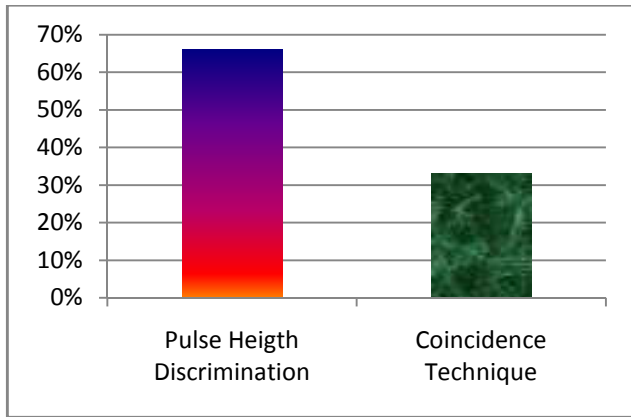


Figure 15: The technique suitable to determine efficiency of detectors from students rating of their opinion

The two techniques i.e. pulse height discrimination and coincidence technique when compared for determining the efficiency of detectors (as shown in graph (figure 15)), 66% of the students opted for pulse height discrimination where as 33% opted for coincidence technique.

11. Among the equipments given, which can cause main source for errors/noise in the experiment?

- a. Scintillator
- b. Coaxial Cables
- c. PMT
- d. Discriminator

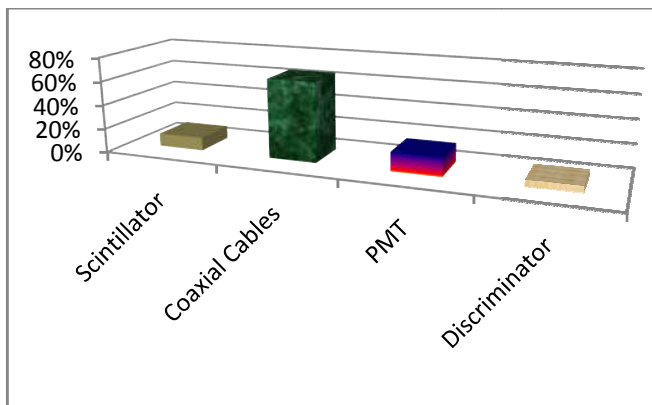


Figure 16: Students feedback regarding the noise/error source in experiment within the equipments

When discussed for possible error/noise source in experiment as shown in graph (figure 16)), 66% of the students gave their feedback for coaxial cables and 16% opted for PMT as a main source of noise in experiment.

4. Review on Previous Studies Done:

4.1 Time Characteristics studies of PMT:

The dynode voltage drops in different Photo Multiplier Tubes with respect to PIN number have been tested on fixing H.V of PMT for long time. The most important factor in any timing system is its resolution. One method is to measure the resolution i.e. to measure the time difference of two exactly coincident signals [33]. The *walk* effect occurs due to variations in the amplitude and/or rise time of the incoming signals. For example, even though if two signals of different pulse amplitude is in coincident, then the two signals will trigger the discriminator at different position. The second cause of walk effect is the charge required to trigger the leading edge of the pulse. Noise and statistical fluctuations also result in a time variation of signals generally termed as time jitter.

4.2 Efficiency Studies of Scintillation Counters:

Instead of measuring the number of particles passing through the detector, efficiency of the entire system can be determined from the coincidence measurement. The ratio of coincidence counters to optimized counters allows to study the number of particles in a particular counter detects relative to the others.

The efficiency is calculated from the plateau region of third paddle (3F/2F) (Detector dimension is $60 \times 20 \times 1 \text{ cm}^3$, $45 \times 3 \times 1 \text{ cm}^3$, $45 \times 2 \times 1 \text{ cm}^3$). It is studied as function of longitudinal length of the detector and also with respect to varying distance from PMT (Detector dimension is $199 \times 19.5 \times 0.9 \text{ cm}^3$) [34]. The Plateau region of the test paddle determined from the efficiency (3F) (1st paddle = $200 \times 165 \times 10 \text{ mm}^3$, 2nd paddle = $200 \times 165 \times 10 \text{ mm}^3$, Test paddle = $340 \times 200 \times 10 \text{ mm}^3$) [35]. Probability at a certain time instant where all four paddles record a signal was

calculated from the individual count rate per 100 sec, 4-fold trigger rate per 600 sec and average frequency (Hz). Here the chance coincidence in which a muon passes through paddles 1, 3, 4 and paddle 2 records any signal (noise/muon) also determined along with actual chance coincidence rate, actual cosmic ray muon rate and average muon flux (P1 – $30 \times 2 \times 1 \text{ cm}^3$, P2 – $30 \times 3 \times 1 \text{ cm}^3$, P3 – $40 \times 20 \times 1 \text{ cm}^3$, P4 – $40 \times 20 \times 1 \text{ cm}^3$)[36]. Efficiency (counts/hr) rate taken for two weeks where the correlation between count rate and atmospheric pressure, temperature, barometric coefficient within 2 weeks observed. The statistics such as chi-square test, p-value, correlation coefficient, slope of the correlation was also determined ($1000 \times 200 \times 10 \text{ mm}^3$ with $2 \times 2 \text{ mm}^3$ square type WLS fibre)[37].

4.3 Calibration of TDC:

The time scale of TDC was calibrated in work conducted from reference [38]. Distance between the peaks produced by different delays and the time resolution of the paddles ($60 \times 20 \times 1 \text{ cm}^3$, $45 \times 3 \times 1 \text{ cm}^3$, $45 \times 2 \times 1 \text{ cm}^3$) were measured.

4.4 Calibration of ADC:

In the report [38], number of photoelectrons produced at the PMT photocathode from scintillator paddle for cosmic ray muon ($60 \times 20 \times 1 \text{ cm}^3$, $45 \times 3 \times 1 \text{ cm}^3$, $45 \times 2 \times 1 \text{ cm}^3$) was measured. Muon energy was determined (P1 – $30 \times 2 \times 1 \text{ cm}^3$, P2 – $30 \times 3 \times 1 \text{ cm}^3$, P3 – $40 \times 20 \times 1 \text{ cm}^3$, P4 – $40 \times 20 \times 1 \text{ cm}^3$). Response spectrum on changing the coincidence width was also studied for Number of counts v/s ADC channel ($1000 \times 200 \times 10 \text{ mm}^3$ with $2 \times 2 \text{ mm}^3$ square type WLS fibre from).

4.5 Radioactive source:

The isotropic behavior of radiation using two detectors where one is fixed at a position and other is varied at different angles – coincidence counts. Study the inverse square law behavior. Study the dependence of cosmic ray flux on placing different shielding (lead, Al, wood) between

source and PMT (Lead acid battery – 6.35 cm, Al – 0.3175 cm thick, Wood – 5.08 cm) [39].

4.6 Atmospheric parameters:

The correlation between the flux distributions and barometric pressure was studied with variable angular acceptance at the earth's surface of two scintillator paddle muon telescope. A paddle separation of 0, 7, 14 inches conducted for a correlation and anti-correlation analysis of muon count rate with the barometric pressure, surface temperature, stratospheric temperature and solar activity parameters (IMF (nT), plasma speed (km/hr) and Kp index) ($33 \times 7 \times 1 \text{ cm}^2$, $12 \times 12 \text{ cm}^2$) [40]. The dependence of cosmic ray flux over zenith and azimuthal angle observed. Coincidence counts as function of shielding thickness was also determined (Three scintillator – $40 \times 80 \times 3 \text{ cm}^2$, Light guide – $40 \times 40 \text{ cm}^2$, Iron plate – 2cm thick) [40].

5. Conclusion:

Cosmic rays are a prevailing source of information for performing high energy physics experiments. They provide energetic, correlated, particles which arrive on Earth. The detection of such particles and the study of the inclusive and definite properties of secondary cosmic rays may provide basic and advanced educational activities to get involved of undergraduate and post graduate students. The hardware required by such experiments may include the use of scintillators and fast pulse techniques for possible experimental investigations. By such devices we can carry out numerous quantitative experiments, with the prospect to enhance the physics curriculum.

6. Future Plans:

Students are presently performing horizontal coincidence, vertical coincidence and at different elevations. Later they are going to compare the difference among the count rate of horizontal and vertical coincidence. They will also determine the efficiency of detectors from three fold and four fold. The effect of absorbers when placed between

detectors will be observed from their count rate. Future plan is to interface with CAEN C111C Ethernet CAMAC Controller, calibrating Phillips TDC 7187 and Phillips 7164 ADC module to study the resolution which have an impact on range of digitization and time spectrum of the particle. Measure and store the time difference between the two pulses generated in the same detector to visualize the two pulses originating from the muon and the electron. Investigate the cosmic ray muon life time with different counters and absorbers.

7. Acknowledgment:

The authors wish to thank Cosmic Ray Laboratory (CRL), Field Station of Tata Institute of Fundamental Research, Ooty; for its technical assistance in fabricating and designing the plastic scintillation detectors. We want to express special thanks to Prof. Sunil Gupta, Shri K.C Ravindran, Shri. Atul Jain, Shri. C. Ravi and to the staff, management of Cosmic Ray Laboratory, Ooty.

The authors also thank Panjab University, Inter University of Accelerator Center for their technical assistance in setting up data acquisition. We want to express special thanks to Dr. Vipin Bhatnagar, Shri. V.K Bhandari, Shri. Kundan Singh, Mrs. Ruby Santhi and Shri.V.V.V Satyanarayana.

8. References:

- [1] Sonali Bhatnagar et.al, “Preliminary Studies of muon telescope”, 31st National Conference of Indian Association for Radiation Protection on “Advances in Radiation Measurement Systems and Techniques”, March 19-21, 2014, BARC, Mumbai.
- [2] Sonali Bhatnagar, “High Energy Cosmic Rays”, Indian Association of Physics Teachers Bulletin, Vol.24, No.11, pp 336, Nov. 2007.
- [3] Sonali Bhatnagar, “Extensive Air Shower-High Energy Cosmic Rays (II)”, Physics Educational Journal, University of Pune, Oct-Dec 2009.
- [4] Sonali Bhatnagar, “Gamma Ray astronomy at PeV energies”, Current Science, Vol. 97, No 7, 10 October, 2009.
- [5] Bogdanov, A.. “Energy spectrum of cosmic ray muons in ~100 TeV energy region reconstructed from the BUST data”, *Astroparticle physics*, 224, 2012.
- [6] Ralph Engel, “Extensive Air Showers and Hadronic Interactions at High Energy”, *Annu. Rev. Nucl. Part. Sci.* 2011, 61: 467-489.
- [7] Pasquale Blasi, “Theoretical challenges in acceleration and transport of ultra-high energy cosmic rays: A review”, *EDP sciences*, 53, 01002 (2013).
- [8] James J. Beatty, “The Highest Energy Cosmic Rays”, *Ann. Rev. Nucl. Part. Sci.* 59, 319-45, 2009.
- [9] Watson. A. A, “Recent results from the Pierre Auger Observatory—Including comparisons with data from AGASA and HiRes”, *Nuclear Instruments and Methods in Physics Research Section A*, Volume 588, Issue 1-2, p. 221-226.
- [10] Muons in air showers at the Pierre Auger Observatory: Measurement of atmospheric production dept, *Physical Review D*, 90 (2014) 012012 arXiv: 1407.5919.
- [11] T. Yamamoto, “Development of Atmospheric Monitoring System at Akeno Observatory for the Telescope Array

- Project”, Nucl.Instrum.Meth. A488 (2002) 191-208.
- [12] Mattia di Mauro, “New evaluation of the antiproton production cross section for cosmic ray studies”, Phys. Rev. D 90, 085017 – Published 20 October 2014
- [13] P. Abru, “The Pierre Auger Observatory II: Studies of Cosmic Ray Composition and Hadronic Interaction models”, arXiv:1107.4804 [astro-ph.HE].
- [14] S Riggi, “A large area cosmic ray detector for the inspection of hidden high-Z materials inside containers”, 2013 *J. Phys.: Conf. Ser.* 409
- [15] D.J Thomson, “Cosmic ray studies with the Fermi Gamma-ray Space Telescope Large Area Telescope”, Cosmic rays topical issue, Volumes 39–40, December 2012, Pages 22–32.
- [16] V. Berezhinsky, “Dip in UHECR spectrum as signature of proton interaction with CMB arXiv:astro-ph/0502550v1 28 Feb 2005
- [17] R. Aloisio, Ultra High Energy Cosmic Rays: The disappointing model, arXiv:0907.5194v2 [astro-ph.HE] 16 Feb 2011
- [18] D. Allard, UHE nuclei propagation and the interpretation of the ankle in the cosmic-ray spectrum, arXiv:astro-ph/0505566v2 4 Jun 2005
- [19] D. Kosenko, “Parametric studies of cosmic ray acceleration in supernova remnants”, MNRAS (September 11, 2014) 443(2): 139 0-1401.
- [20] Lazarian, “Heliotail and anisotropy of cosmic ray flux”, 40th COSPAR Scientific Assembly. Held 2-10 August 2014, in Moscow, Russia, Abstract D1.4-6-14.
- [21] A.A.Petrukhin., “Muon puzzle in cosmic ray experiments and its possible solution.” *Nuclear Instruments and Methods in Physics Research A* , 228-231, 2014.
- [22] Gupta, S, “High Energy Astroparticle Physics at Ooty and the GRAPES-3 Experiment”, *Proc Indian Natn Sci Acad* , 80 No. 4, pp. 827-876, 2014.
- [23] Dayananda, M. A., “Correlation Studies of Cosmic Ray Flux and Atmospheric and Space Weather”. *ScholarWorks @ Georgia State University*, 2013.
- [24] B'en', S., “Air shower simulation for background estimation in muon tomography of volcanoes”. *Geosci. Instrum. Method. Data Syst* , 11-15, 2013.
- [25] Overholt, A. C. “A link between solar events and congenital malformations: Is ionizing radiation??”, 2015.
- [26] Cortes, M. L., BC404 scintillators as gamma locators studied via Geant4 simulations. *Journal of Instrumentation* , JINST 9 C05049, 2014.
- [27] Leo, W.R; (1994) Techniques for Nuclear and Particle Physics Experiments, Second Revised edition, Berlin Heidelberg: Springer-Verlag.
- [28] Glenn F. Knoll, “Light Collection in scintillation detector composites for neutron detection”, IEEE Transactions on Nuclear Science, Vol. 35, No. 1, February 1988
- [29] Data Sheet Manual, Quad 300 MHz Discriminator, Model 704, Phillips Scientific
- [30] Data Sheet Manual, Quad Four Fold Logic Unit, Model 756, Phillips Scientific

-
- [31] Data Sheet Manual, Quad Scaler Preset Counter and Timer, Model N1145, CAEN. Environmental Center”, *Advances in Space Research* 47 (2011) 1140–1146.
- [32] Mitrica, B., “A Mobile Detector for Muon Measurements Based on Two Different Techniques”. *Advances in High Energy Physics*, 1-7, 2013.
- [33] Yun Ho Kim, “Cosmic ray measurement and experimental temperature analysis with a muon detector”, *Journal of Korean Physical Society*, Vol. 64, No:4 August 2012, Pg:647-652.
- [34] Cecchini., “Atmospheric muons: experimental aspects”. *Geosci. Instrum. Method. Data Syst*, 185-196, 2012.
- [35] Riggi, S., “Muon tomography imaging algorithms for nuclear threat detection inside large volume containers with the Muon Portal detector”. *Nuclear Instruments and Methods in Physics Research A*, 59, 2013.
- [36] MAGHRABI., “Future Plans for Cosmic Ray Activities in Saudi Arabia”. *33RD INTERNATIONAL COSMIC RAY CONFERENCE*, 1-3, 2013.
- [37] Hofverberg, P, “Cosmic ray anisotropy studies with the Stockholm Educational 1-5, 2011.
- [38] A.Ollila, “Changes in cosmic ray fluxes improve correlation to global warming”, *International Journal of the Physical Sciences*, 822-826, 2012.
- [39] A. Dragic, “Measurement of cosmic ray muon flux in the Belgrade ground level and underground laboratories”, *Nuclear Instruments and Methods in Physics Research A* 591 (2008) 470–475.
- [40] A. Chilingarian, “Calculation of the barometric coefficients at the start of the 24th solar activity cycle for particle detectors of Aragats”, *Space*
-